Percolation in cluster-cluster aggregation processes

Anwar Hasmy[1,2] and Rémi Jullien[1]
[1]*Laboratoire de Science des Matériaux Vitreux, UA 1119 CNRS, Université Montpellier II, Place Eugène Bataillon, 34095 Montpellier Cedex 5, France*
[2]*Laboratoire de Physique des Solides, Université Paris-Sud, Centre d'Orsay, 91405 Orsay, France*
(Received 11 April 1995; revised manuscript received 27 June 1995)

Numerical simulations of diffusion-limited and reaction-limited cluster-cluster aggregation processes of identical particles are performed in a two-dimensional box. It is shown that, for concentrations larger than a characteristic gel concentration, the morphology of the resulting spanning cluster at the gel time t_g exhibits a crossover length L_c between percolation ($l > L_c$) and aggregation ($l < L_c$). L_c vanishes when increasing c, and, at a critical concentration value $c_p \simeq 0.5$ (where $L_c \to 0$) the entire spanning cluster scales as the percolating cluster obtained by standard percolation. Even if for $0.5 < c < 0.8$ the long-range correlations seem to be similar to that of percolation, the scaling mass analysis and the vanishing links in the structure suggest that a homogeneous regime appears at small scales.

PACS number(s): 61.43.Hv, 64.60.Ak

I. INTRODUCTION

The aggregation processes of small particles have attracted great theoretical interest in the last decade [1–4], due to their wide range of applications. One can distinguish particle-cluster aggregation, whose prototype is the Witten-Sander model [5], and cluster-cluster aggregation (CCA) [6,7]. While the former model applies to field-induced growth processes, such as electrodeposition [8,9], dielectric breakdown [10], viscous fingering [11,12], etc., the latter explains true aggregation processes such as polymerization [13,14], oil in water emulsions [15], soot particles in flames [16], and flocculation of colloidal particles [17–21]. Among cluster-cluster aggregation processes one distinguishes diffusion-limited cluster-cluster aggregation (DLCA) [6,7] and chemically limited (also called reaction-limited) aggregation (RLCA) [22–24], which correspond, respectively, to fast (fully screened) and slow (partially screened) aggregation of colloids [17].

The CCA processes lead to a flocculation regime when the concentration is smaller than a characteristic gel concentration c_g, and to a gelation regime otherwise. In a flocculation regime it remains a single fractal cluster at the end of the aggregation process with a fractal dimension D equal to 1.45 in the DLCA case (and 1.65 in the RLCA case). In the gelation regime it appears as an "infinite" cluster at a given time t_g (hereafter referred to as the gelling cluster). When working with a finite (but large) box, such a cluster is usually defined as touching the box from edge to edge as in the percolation theory [25]. Since both of the physical problems are quite similar, it is tempting to explain the infinite cluster formation in DLCA by the percolation theory, which excludes all dynamical phenomena, and this has been done by several authors [26–31]. The fractal dimension of the infinite cluster of DLCA has been found to be different than the one of percolation [26,27], and it has been argued that this discrepancy is due to dynamical effects. However, recently aggregation experiments [32] on attractive coagulated particles suggest that percolation transition occurs at the particle concentration 0.42. Also, in an interesting recently published paper, Gimel *et al.* [31] argue that percolation and the DLCA model are equivalent at high concentration, but they do not consider periodic boundary conditions. Therefore the question is still open: are CCA models and percolation theory compatible?

In this paper we show that the infinite cluster obtained at t_g in CCA models exhibits a crossover length L_c between percolation and aggregation, for concentration values c larger than the gel concentration c_g. Furthermore, we show that L_c vanishes when increasing c, and for $c \approx 0.5$ the percolation regime shows up at all length scales in the infinite cluster. These results suggest that CCA processes can be viewed as an irreversible percolation phenomenon, as the invasion percolation model without trapping [33,34] and the model for a diffusion front [35].

II. THE MODEL

The two-dimensional diffusion-limited cluster-cluster aggregation model consists of a Monte Carlo algorithm that builds clusters on a lattice within a square box of edge length L. Initially particles are distributed randomly (but uniformly in the space) on the lattice sites up to volume fraction (concentration) c. In order to insure that the diffusion coefficient of the clusters varies as the inverse of their radius R, a particle (or a cluster containing n_i particles) is chosen randomly according to a probability,

$$p_{n_i} = \frac{n_i^\alpha}{\sum_j n_j^\alpha} , \tag{1}$$

where α ($=-1/D$) is the kinetical exponent. Then the cluster performs a translational motion by one unit [taking into account periodic boundary conditions (PBC)] in any of the four directions $\pm 1, \pm 1$ chosen at random. If the cluster does not collide with another, the displacement is performed and the algorithm goes on by choosing again another cluster. If a collision occurs between two clusters they stick together, forming a new large cluster. In our simulation we have considered that collision occurs when a particle of a cluster tries to occupy a particle of another cluster. In that case the cluster is not displaced but a bond is established between the two contacting particles. If there is more than one collision at a given motion, only one bond is chosen at random. This trick was used by Kolb in a reversible diffusion-limited cluster aggregation model [28]. This important variant implies that there are no loops (as in off-lattice DLCA [36]) and that there is no intrinsic percolation at the beginning of the process: the intitial concentration can be varied up to unity.

For concentrations larger than c_g there exists a gel time t_g where a cluster becomes infinite. This gelling cluster is stored for a numerical analysis, and to compare, we leave the aggregation process continuing up to the time where it remains only one cluster (hereafter referred to as the final cluster). In the case of reaction-limited cluster-cluster aggregation [22–24], in addition to the algorithm described above, a sticking probabilty is introduced, $p(\ll 1)$. After a collision a new bond is created only if a random number (uniformly distributed between zero and one) is smaller than p. Here, we have performed two-dimensional simulations in boxes of different sizes up to $L = 240$.

III. RESULTS AND DISCUSSION

Typical results that qualitatively compare the resulting morphologies of the gelling cluster (G) and the final cluster (F) in DLCA are illustrated in Fig. 1. In the case of the gelling cluster the other remaining clusters have been discarded and therefore are not shown. Note that the morphology of the cluster shown in Fig. 1(a) is strongly reminiscent of that of a percolating cluster,

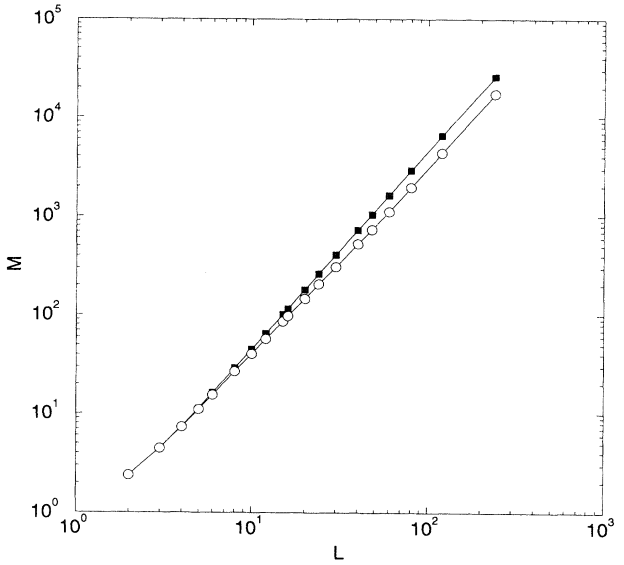

FIG. 2. Log-log plot of M versus l for c=0.5 and L=240, for the gelling cluster G (open circles) and the final cluster F (black squares). These curves result from the averages of over 40 simulations.

as obtained in standard percolation theory [25] when occupying randomly the sites of a square lattice with the percolation probability $p_c = 0.592\,73$. To make quantitative comparisons between G and F, we have calculated the mass M dependent box size l using the mass-counting algorithm [37]. In Fig. 2 we show the log-log plot of M versus l for the same concentration of those considered in Fig. 1. The resulting slope indicates that M scales as l^{D_p} and l^d, for G (open circles) and F (black squares), respectively. D_p (=1.89) is close to the fractal dimension of the percolating cluster in two dimensions, and d(=2) is the spatial dimension.

If the mass of the gelling cluster G or the mass of the final cluster F scales as l^D we might be tempted to conclude that the quantity $m = M(l)/cl^D$ should not depend on l. To test this we show, in Fig. 3, the curves giving m as a function of l. Figures 3(a) and 3(c) correspond to G

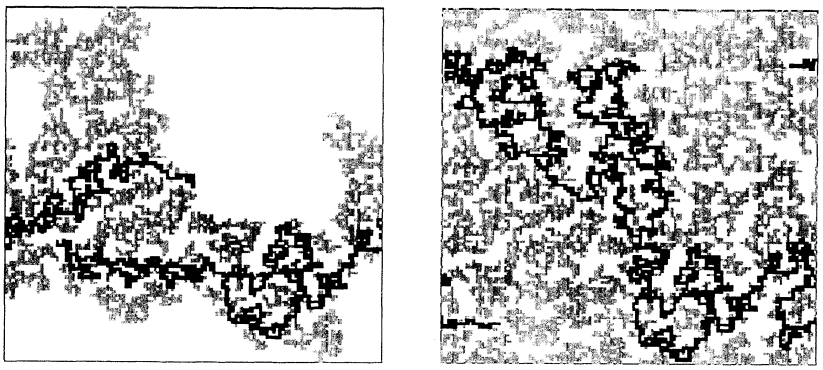

FIG. 1. Typical configurations for a (a) gelling cluster G and (b) final cluster F, for $c = 0.5$ and $L = 120$. The sites shown in dark grey and black belong to the backbone and the links, respectively.

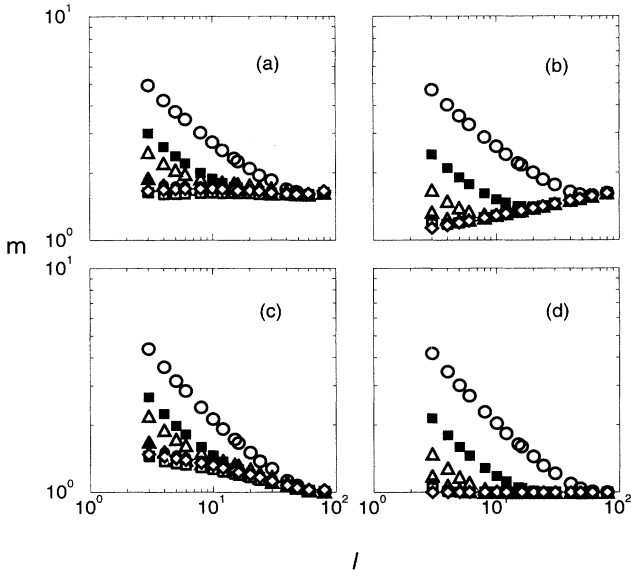

FIG. 3. Log-log plot of $m[= M(l)/l^D]$ versus l for $L = 240$ and different concentration values (0.1, 0.2, 0.3,..., 0.7, from top to bottom) in the DLCA case. (a) and (c) correspond to the G cluster for $D = D_p$ and $D = d$, respectively. (b) and (d) correspond to the F cluster for $D = D_p$ and $D = d$, respectively. These curves result from the averages of over 40 simulations.

for $D = D_p$ and $D = d$, respectively, and Figs. 3(b) and 3(d) correspond to F for $D = D_p$ and $D = d$, respectively. At large l values one observes in these figures that m is independent of l only in cases 3(a) and 3(d) and for sufficiently large concentrations, confirming our first guess of different fractal dimensions, 1.89 and 2.00, for G and F, respectively. Figures 3(b) and 3(c) are shown here as counterexamples to illustrate the high precision of these estimates for the fractal dimensions. In general, i.e., for concentrations that are not too large, one can define a c-dependent crossover length L_c such that m becomes independent of l only for $l > L_c$. For $l < L_c$, another linear regime is observed, which is better extended at very low concentration, with a slope of about -0.4 and -0.5 in cases 3(a) and 3(d), respectively, corresponding to the fractal dimension $D \simeq 1.89-0.4 \simeq 2.00-0.5 \simeq 1.5$, close to the one of DLCA clusters. Therefore L_c defines a change of scaling regime between DLCA for short lengths and either percolation (G) or homogeneity (F) for large lengths. In fact, L_c should be proportional to the characteristic length correlation ξ (or average size) of DLCA fractal aggregates [36]. Note that in all cases L_c vanishes for $c \approx 0.5$, and this is the reason for the absence of crossover in the curves reported in Fig. 2. For $c > 0.5$, Fig. 3(c) suggests that in the G cluster a homogeneous regime appears at small scales, since $m(l)$ become to be independent of l for $l \sim< 10$ (see open diamonds: $c = 0.7$). In fact, we have observed that for high concentrations ($c > 0.5$) the homogeneous regime goes up from small scales to long scales, and for $c >\sim 0.8$ the G cluster becomes statistically compact in volume and fractal-like in surface (as those obtained by Kolb and Herrmann [38] for $c = 1$ and $\alpha < 0$).

When estimating the fractal dimension of the aggregates D_{agg} in the range of lengths corresponding to the aggregation regime ($l < L_c$), we found, in both cases G and F, that it increases significantly with concentration (the data are reported in Fig. 4). Those results confirm previous conclusions in two dimensions [39] as well as in three dimensions [40]. As a consequence the c dependence of L_c cannot be analyzed as a simple scaling relation. Moreover, the discrete values of l that require mass-counting calculations and finite size effects impede our ability to determine L_c within a sufficiently small range of error. Anyway, all the results depicted in Figs. 2 and 3 suggest that, at least for $l > L_c$ the mass of the gelling cluster G scales with l as a standard percolation cluster. However, such results are not sufficient to insure that their morphologies are the same. It is well known that there exist additional quantities (different and independent on the fractal dimension) to characterize a percolating cluster. In principle, the morphology is entirely characterized by an infinite set of exponents [25,41], but here we shall focus on three particular exponents: the fractal dimensions of the "backbone" D_{bb} [42], the fractal dimension of the "links" D_l [43], and the fractal dimension of the hull D_H [44]. The backbone of a cluster is the ensemble that remains after removing dead ends (or dangling ends). The links (also called red bonds) are the sites of the cluster that are singly connected; that is, if we take out a link the connection between the entire cluster is broken. The hull, or outer perimeter, is a set of empty sites that is adjacent to the cluster sites; in other words, the hull envelopes the cluster from outside. For a

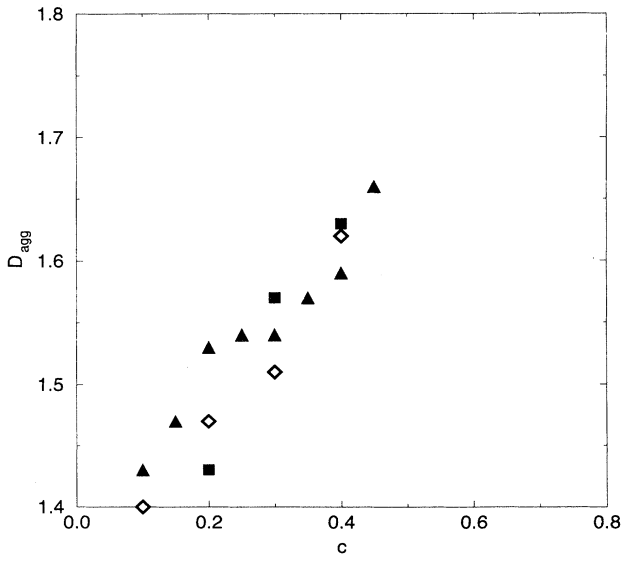

FIG. 4. Fractal dimension of the aggregates D_{agg} ($l < L_c$) versus c, for $L = 90$ (black squares), $L = 120$ (black triangles), and $L = 240$ (open diamonds), resulting from the averages of over 80, 60, and 40 simulations, respectively.

percolating cluster in two dimensions the fractal dimension of the backbone D_{bb}, of the links D_l, and of the hull D_H is equal to 1.61, 0.75, and 1.75, respectively.

In order to identify the backbone, the links, and the hull of a given cluster, we have been obliged (due to the PBC considered in the CCA simulations) to span the cluster out of the box, taking account of PBC. Then, we have applied to the new cluster configuration (with a size larger than the box size L, in almost all situations) a procedure suggested by Herrmann *et al.* [45] to identify the backbone and the links. Finally, the resulting backbone (links and hull) is unspanned and returned inside the original box. In Figs. 1, the sites depicted with dark grey and black colors denote the backbone and the links, repectively.

We have calculated the fractal dimension of the backbone D_{bb} for both G and F clusters and different concentration values. The results are depicted in Fig. 5. Note that for small concentration values the fractal dimension D_{bb} of the backbone, for both G (open circles) and F clusters (black squares), are quite similar and increase for increasing c values. This can be understood, since, as mentioned above, the fractal dimension in the aggregation regime is almost the same in both cases. The increasing value of D_{bb} suggests that the backbone structure is mainly reflecting the fractal aggregate structure (which also increases with concentration, as shown in Fig. 4). For larger c values, D_{bb} of the gelling cluster G becomes smaller than D_{bb} of the final cluster F. In the G case for $c \approx 0.5$, as indicated by the arrow in Fig. 5, D_{bb} reaches the value 1.61 (the same value as for a percolating cluster). In fact, it is only when the crossover length L_c vanishes that the backbone structure becomes characteristic of the one of a percolating cluster. For $c > 0.5$, D_{bb} continues to increase with c, and this can be explained by the homogeneous regime that goes up from small scales to long scales for increased c values (as argued above when we discussed Fig. 3).

In Fig. 6 it is shown that for c smaller than about 0.5, the fractal dimension D_l of the links is approximately equal to 1, suggesting that the mass of the links scales with l in a trivial manner. However, for $c \approx 0.5$ (as indicated by the arrow in Fig. 6), D_l reaches the value 0.75, as in a percolating cluster. The D_l independence of the box size L suggests that there exists a threshold concentration close to 0.5, where the entire G cluster scales exactly as a percolating cluster. When c is increased above this threshold, D_l vanishes. The vanishing links in the gelling cluster for large c values give more evidence that at very small scales, the system becomes homogeneous.

We have calculated the fractal dimension of the hull D_H for different concentration values. The results are depicted in Fig. 7. For $c = 0.1$ we are close to the gel concentration c_g [where the crossover length L_c is practically equal to the box size L, as deduced from Fig. 3(a): see open circles]. The percolation regime does not exist and one can expect that both values for D_H and the fractal dimension of the aggregate ($D_{agg} \approx 1.45$) are approximately the same. In fact, in our numerical calculation we found that $D_H \approx 1.5$. For $0.1 < c < 0.6$ we obtain that D_H is close to the one known for percolation at $p = p_c$ (1.75) [44]. Therefore, one can conclude that, in this range of concentration, D_H is mainly reflecting the percolation regime, in contrast to D_{bb}, which is mainly reflecting the aggregation regime as mentioned above. For $0.5 < c < 0.8$ we found a crossover length in the hull mass

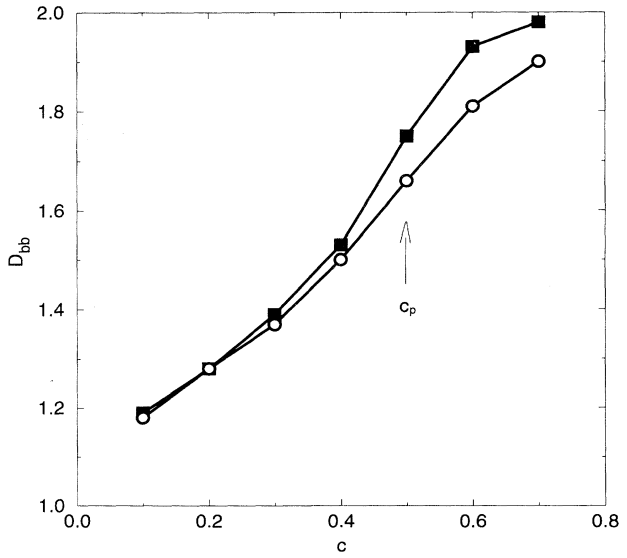

FIG. 5. Fractal dimension of the backbone D_{bb} versus c for $L = 120$. Open circles and black squares denote D_{bb} for the gelling cluster and the final cluster, respectively. These data result from the averages of over 60 simulations.

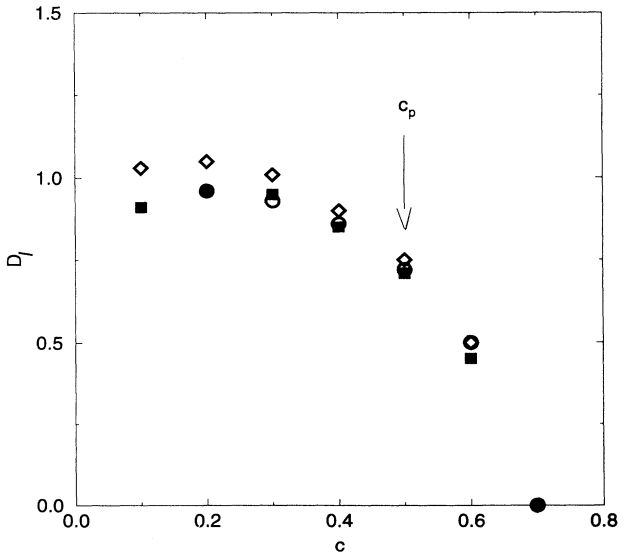

FIG. 6. Fractal dimension of the links D_l versus c for the G cluster, for $L = 60$ (open circles), $L = 90$ (black squares), and $L = 120$ (open diamonds), resulting from the averages of over 120, 80, and 60 simulations, respectively.

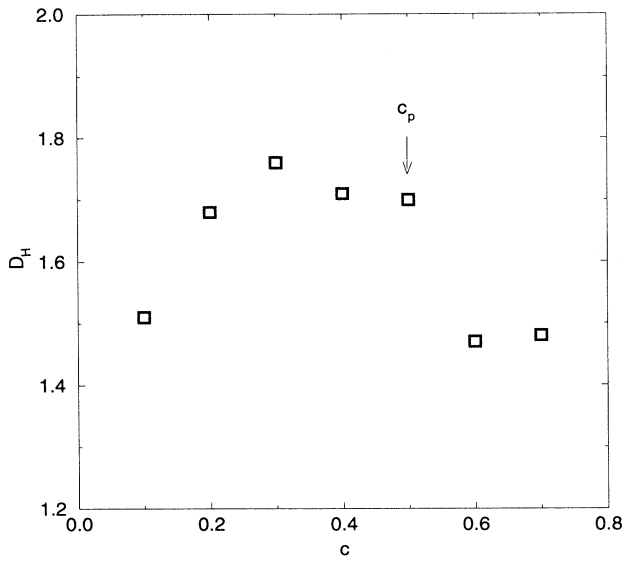

FIG. 7. Fractal dimension of the hull D_H versus c for the G cluster and for $L = 120$. This data results from the averages of over 30 simulations.

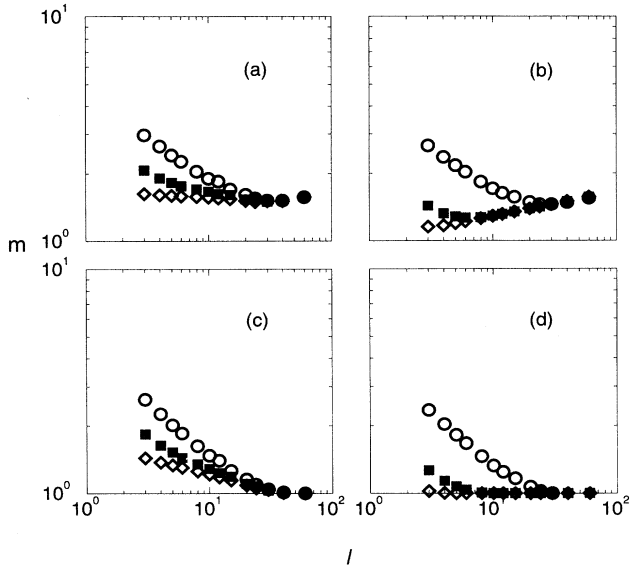

FIG. 8. Log-log plot of $m[= M(l)/cl^D]$ versus l for $L = 120$ and different concentration values (0.2, 0.4, and 0.6, from top to bottom) for the RLCA case (with a sticking probability equal to 0.005). (a) and (c) correspond to the G cluster for $D = D_p$ and $D = d$, respectively. (b) and (d) correspond to the F cluster for $D = D_p$ and $D = d$, respectively. These curves result from the averages of over 20 simulations.

dependent l curves; this crossover has been confirmed by calculations of the correlation function of the gelling cluster. The results reported in Fig. 7 correspond to the bigger l values ($>\sim 8$). This crossover becomes smaller for $c = 0.7$. In fact, we think that for $c > 0.8$, where the system becomes compact in volume, this crossover vanishes, and the fractal dimension of the hull D_H saturates to the value reported here for $c > c_p$, a value (within the estimated errors) close to the one reported by Kolb and Herrmann [38] for $\alpha < 0$ and $c = 1(1.6 \pm 0.8)$.

In order to appreciate the degree of generality of our results, we have also performed some calculations in the reaction-limited case (RLCA). In Fig. 8 we have reported the $m(l)$ curves, and it can be shown that they exhibit the same qualitative behavior as in the DLCA case (Fig. 3). These results suggest that the percolation scaling could exist in other kinds of CCA processes, such as the ballistic-limited [46], the convection-limited [47], and the fluctuating bond [48] aggregation models.

IV. CONCLUSION

In this paper we have shown that the infinite cluster obtained at the gel time t_g in CCA models exhibits a crossover length L_c between aggregation and percolation. Moreover, L_c vanishes at a critical concentration $c_p(\simeq 0.5)$, where the mass of the entire system (and its backbone, hull, and links) scales as for a percolating cluster obtained at p_c. For $c_p < c < 0.8$ the percolation regime persists at least at large scales, because the scaling mass analysis and the vanishing links suggest that a homogeneous regime appears at small scales going up to long scales when increasing c. The value obtained here for c_p is close to the value reported in the above mentioned experimental work [32] ($\simeq 0.42$), but typical statistical fluctuations to determine a critical value impedes our ability to insure if there are some relations between these two critical concentrations. It might also be worth finding a relation between c_p and the critical probability of the site percolation threshold ($p_c = 0.592\,73$) on a square lattice. Preliminary calculations on a cubic lattice suggest that the results reported here are quite general and extend in three dimensions. Moreover, we have performed some preliminary calculations of the cluster size distribution for $d = 2$, and we found that, at c_p, for large clusters the scaling exponent τ of this function is close to the one known for percolation at p_c ($\tau = 2.0549...$). For small cluster sizes we found a smaller exponent ($\tau \approx 1$), but it has been shown [49] that in this domain the exponent depends strongly on the kinetical exponent α, and we think that accurate calculations should be addressed in the future for this range of concentration.

ACKNOWLEDGMENTS

One of us (A.H.) would like to acknowledge support from CONICIT (Venezuela). The numerical calculations were done on the computers of the CNUSC (Centre Universitaire Sud de Calcul), Montpellier, France, with support from CNRS.

[1] F. Family and D. P. Landau, *Kinetics of Aggregation and Gelation* (North-Holland, Amsterdam, 1984).
[2] R. Jullien and R. Botet, *Aggregation and Fractal Aggregates* (World Scientific, Singapore, 1987).
[3] P. Meakin, *Phase Transitions and Critical Phenomena* (Academic, New York, 1988), Vol. 12, p. 335.
[4] T. Vicsek, *Fractal Growth Phenomena* (World Scientific, Singapore, 1989).
[5] T. A. Witten and L. M. Sander, Phys. Rev. Lett. **47**, 1400 (1981).
[6] P. Meakin, Phys. Rev. Lett. **51**, 1119 (1983).
[7] M. Kolb, R. Botet, and R. Jullien, Phys. Rev. Lett. **51**, 1123 (1983).
[8] M. Matsushita, M. Sano, Y. Hayakawa, H. Honjo, and Y. Sawada, Phys. Rev. Lett. **53**, 286 (1984).
[9] J. Mach, F. Mas, and F. Sagués, Europhys. Lett. **25**, 271 (1994).
[10] L. Niemeyer, L. Pietronero, and H. J. Wiesmann, Phys. Rev. Lett. **52**, 1033 (1984).
[11] A. Arnéodo, Y. Couder, G. Grasseau, V. Hakim, and M. Rabaud, Phys. Rev. Lett. **63**, 984 (1989).
[12] H. La Roche, J. F. Fernández, M. Octavio, A. G. Loeger, and C. J. Lobb, Phys. Rev. A **44**, 6185 (1991).
[13] B. Cabane, M. Dubois, and R. Duplessix, J. Phys. (Paris) **48**, 2131 (1987).
[14] J. C. Pouxviel, J. P. Boilot, A. Dauger, and A. Wright, J. Non-Cryst. Solids **103**, 331 (1988).
[15] J. Bibette, T. G. Mason, H. Gang, and D. A. Weitz, Phys. Rev. Lett. **69**, 981 (1992).
[16] J. Cai, N. Lu, and C. M. Sorensen, Langmuir **9**, 2861 (1993).
[17] D. A. Weitz, J. S. Huang, M. Y. Lin, and J. Sung, Phys. Rev. Lett. **53**, 1657 (1984).
[18] M. L. Broide and R. J. Cohen, Phys. Rev. Lett. **64**, 2026 (1990).
[19] M. Foret, J. Pelous, and R. Vacher, J. Phys. (France) I **2**, 791 (1992).
[20] D. J. Robinson and J. C. Earnshaw, Phys. Rev. Lett. **71**, 715 (1993).
[21] C. Allain, M. Cloitre, and M. Wafra, Phys. Rev. Lett. **74**, 1478 (1995).
[22] R. Jullien and M. Kolb, J. Phys. A **17**, L639 (1984).
[23] M. Kolb and R. Jullien, J. Phys. Lett. **45**, L977 (1984).
[24] W. Brown and R. C. Ball, J. Phys. A **18**, L517 (1985).
[25] D. Stauffer, *Introduction to Percolation Theory* (Taylor and Francis, London, 1985).
[26] M. Kolb and H. J. Herrmann, J. Phys. A **18**, L435 (1985).
[27] H. J. Herrmann and M. Kolb, J. Phys. A **19**, L1027 (1986).
[28] M. Kolb, J. Phys. A **19**, L263 (1986).
[29] P. Jensen, P. Melinon, A. Hoareau, J. X. Hu, B. Cabaud, M. Treilleux, E. Bernstein, and D. Guillot, Physica A **185**, 104 (1992).
[30] T. Nicolai, D. Durand, and J. C. Gimel, Phys. Rev. B **50**, 16357 (1994).
[31] J. C. Gimel, D. Durand, and T. Nicolai, Phys. Rev. B **51**, 11348 (1995).
[32] Q.-H. Wei, M. Han, C.-H. Zhou, and N.-B. Ming, Phys. Rev. E **49**, 4167 (1994).
[33] D. Wilkinson and J. Willemsen, J. Phys. A **16**, 3365 (1983).
[34] R. Paredes and M. Octavio, Phys. Rev. A **46**, 994 (1992).
[35] B. Sapoval, M. Rosso, and J. F. Gouyet, J. Phys. Lett. **46**, L149 (1985).
[36] A. Hasmy, E. Anglaret, M. Foret, J. Pelous, and R. Jullien, Phys. Rev. B **50**, 6006 (1994).
[37] J. Feder, *Fractals* (Plenum, New York, 1988).
[38] M. Kolb and H. J. Herrmann, Phys. Rev. Lett. **59**, 455 (1987).
[39] H. F. van Garderen, W. H. Dokter, T. P. M. Beelen, R. A. van Santen, E. Pantos, M. A. J. Michels, and P. A. J. Hilbers, J. Chem. Phys. **102**, 480 (1995).
[40] A. Hasmy and R. Jullien, J. Non-Cryst. Solids **186**, 342 (1995).
[41] M. B. Isichenko, Rev. Mod. Phys. **64**, 961 (1992).
[42] H. J. Herrmann and H. E. Stanley, Phys. Rev. Lett. **53**, 1121 (1984).
[43] R. Pike and H. E. Stanley, J. Phys. A **14**, L169 (1981).
[44] R. M. Ziff, Phys. Rev. Lett. **56**, 545 (1986).
[45] H. J. Herrmann, D. C. Hong, and H. E. Stanley, J. Phys. A **17**, L261 (1984).
[46] R. C. Ball and R. Jullien, J. Phys. Lett. **45**, L1031 (1984).
[47] P. B. Warren, R. C. Ball, and A. Boelle, Europhys. Lett. **29**, 339 (1995).
[48] R. Jullien and A. Hasmy, Phys. Rev. Lett. **74**, 4003 (1995); **75**, 24 541(E) (1995).
[49] P. Meakin, T. Vicseck, and F. Family, Phys. Rev. B **31**, 564 (1985).

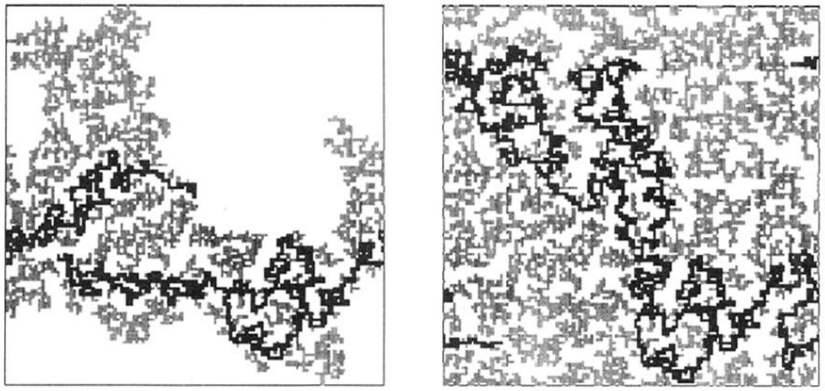

(a) (b)

FIG. 1. Typical configurations for a (a) gelling cluster G and (b) final cluster F, for $c = 0.5$ and $L = 120$. The sites shown in dark grey and black belong to the backbone and the links, respectively.